SUPPORTING INFORMATION

Molecular Weight Dependent Structure and Charge Transport in MAPLE-deposited Poly(3-hexylthiophene) Thin Films

Ban Xuan Dong,[1,┼,] Mitchell Smith,[2] Joseph Strzalka,[3] Huanghe Li,[4] Anne McNeil,[2,4] Gila E. Stein[5] and Peter F. Green[1,4,⊥,*]*

[1]Department of Materials Science and Engineering, Biointerfaces Institute, [2]Department of Chemistry, [4]Macromolecular Science and Engineering, University of Michigan, Ann Arbor, MI 48109, USA

[3]X-Ray Science Division, Argonne National Laboratory, Argonne, Illinois, 60439, USA

[5]Department of Chemical and Biomolecular Engineering, University of Tennessee, Knoxville, TN 37996, USA

[⊥]National Renewable Energy Laboratory, 15013 Denver W Pkwy, Golden, CO 80401, USA.

[┼]Current Address: Institute for Molecular Engineering, The University of Chicago, Chicago, IL, 60637, USA

Correspondence to: Ban Xuan Dong (Email: banxdong@umich.edu) and Peter F. Green (Email: pfgreen@umich.edu).

1) Polymer synthesis

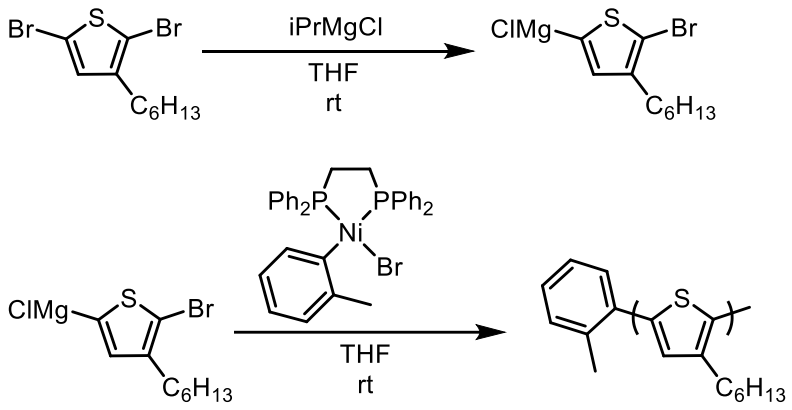

Scheme S1: Synthesis scheme of P3HT

Representative procedure for monomer activation:

In a 20 mL vial in a glovebox, 2,5-dibromo-3-hexylthiophene (2.17 g, 6.65 mmol, 1.00 eq) was dissolved in THF (8.9 mL). n-Docosane (48.7 mg) was added as an internal standard. Isopropylmagnesium chloride (2.84 mL, 2.0M in THF, 0.856 eq) was injected, and the reaction solution was stirred at rt for 30 min. The resulting monomer solution's concentration was determined by titration with salicylaldehyde phenylhydrazone, and was then used in polymerizations.

Polymerization procedures:

In a 20 mL vial in a glovebox, thiophene monomer (2.5 mL, 0.50M in THF, 1.25 mmol, 18 eq) was diluted with THF (17 mL), then rapidly added to a suspension of Ni(dppe)Cl_2 (36.3 mg, 0.0688 mmol, 1 eq) in THF (1 mL) in a 50 mL Schlenk flask. After 30 minutes, the reaction solution was removed from the glovebox and quenched by pouring into $HCl_{(aq)}$ (5 ml, 5M). Organic products were extracted with $CHCl_3$ (15 mL), then precipitated from $CHCl_3$/MeOH. The polymer was then collected on filter paper and subjected to Soxhlet extraction with, sequentially,

MeOH, acetone, and $CHCl_3$. The $CHCl_3$ fractions yielded 221.7 mg of a dark purple solid. M_n = 2.8 kDa, Đ = 1.3.

In a 20 mL vial in a glovebox, thiophene monomer (2.5 mL, 0.50M in THF, 1.25 mmol, 36 eq) was diluted with THF (18 mL), then rapidly added to a suspension of $Ni(dppe)Cl_2$ (18.3 mg, 0.0277 mmol, 1 eq) in THF (1 mL) in a 50 mL Schlenk flask. After 30 minutes, the reaction solution was removed from the glovebox and quenched by pouring into $HCl_{(aq)}$ (5 ml, 5M). Organic products were extracted with $CHCl_3$ (15 mL), then precipitated from $CHCl_3$/MeOH. The polymer was then collected on filter paper and subjected to Soxhlet extraction with, sequentially, MeOH, acetone, and $CHCl_3$. The $CHCl_3$ fractions yielded 148.3 mg of a dark purple solid. M_n = 4.7 kDa, Đ = 1.3.

In a 20 mL vial in a glovebox, thiophene monomer (2.5 mL, 0.48M in THF, 1.2 mmol, 36 eq) was diluted with THF (6.5 mL). A solution of Ni(dppe)tolBr (1 mL, 0.033M, 0.033 mmol,1 eq) was rapidly injected to the monomer solution. After 90 minutes, the reaction solution was removed from the glovebox and quenched by pouring into HCl(aq) (5 ml, 5M). Organic products were extracted with $CHCl_3$ (15 mL), then precipitated from CHCl3/MeOH. The polymer was then collected on filter paper and subjected to Soxhlet extraction with, sequentially, MeOH, acetone, hexanes, and $CHCl_3$. The $CHCl_3$ fractions yielded mg of a dark purple solid. M_n = 10.8 kDa, Đ = 1.4

In a 20 mL vial in a glovebox, thiophene monomer (2.5 mL, 0.48M in THF, 1.2 mmol, 60 eq) was diluted with THF (6.5 mL). A solution of Ni(dppe)tolBr (1 mL, 0.020M, 0.020 mmol,1 eq) was rapidly injected to the monomer solution. After 90 minutes, the reaction solution was removed from the glovebox and quenched by pouring into $HCl_{(aq)}$ (5 ml, 5M). Organic products

were extracted with $CHCl_3$ (15 mL), precipitated from $CHCl_3$/MeOH, and analyzed by GC and GPC. M_n = 12.7 kDa, Đ = 1.3. The polymer was then collected on filter paper and subjected to Soxhlet extraction with, sequentially, MeOH, acetone, hexanes, DCM, and $CHCl_3$. The $CHCl_3$ fraction yielded 118.8 mg of a dark purple solid. M_n = 21.5 kDa, Đ = 1.3

Polymer molecular weights were determined by comparison with polystyrene standards (Varian, EasiCal PS-2 MW 580–377,400) at 40 °C in THF on a Malvern Viscotek GPCMax VE2001 equipped with two Viscotek LT-5000L 8 mm (ID) × 300 mm (L) columns and analyzed with Viscotek TDA 305 (with RI, UV-PDA Detector Model 2600 (190–500 nm), RALS/LALS, and viscometer). All presented data correspond to the absorbance at 254 nm. Samples were dissolved in THF (with mild heating), and passed through a 0.2 μm PTFE filter prior to analysis.

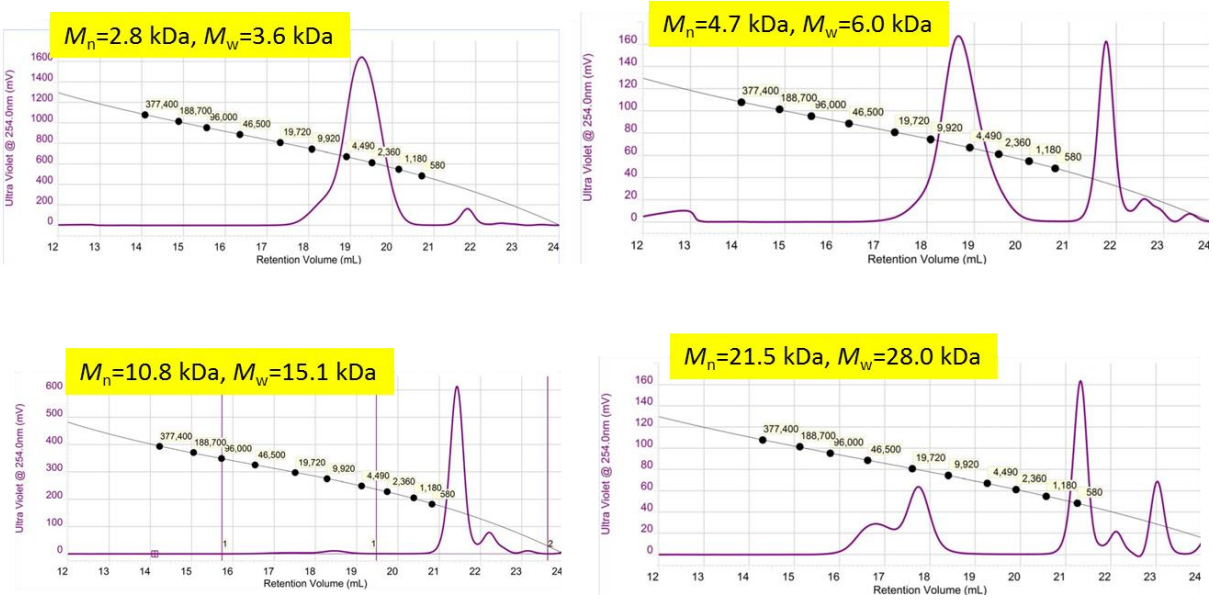

Figure S1: GPC traces of the four polymer batches

2) Williamson-Hall analysis of crystallite size and disorder parameter

To calculate the average crystallite size along the side-chain (100) direction for each sample, in the first step we perform wedge-cut along the vertical direction (phi = 0^0). After appropriate background subtraction, we then fit the (100), (200) and (300) peaks to Voigt functions in order to find full width at half maximum (FWHM) of the peaks. It has been pointed out that the broadening of a Bragg peak in GIWAXS measurement could originate from instrumental resolutions, and the overall broadening is dominated by the geometric smearing effect.[1,2] Thus prior to Williamson-Hall analysis, we correct the geometric effect for each (*h*00) peak according to:

$$\Delta B_{geo} = \frac{w tan(2\theta)}{L} \quad (1)$$

$$\Delta q_{res} \approx \frac{4\pi}{\lambda} \cos(\frac{2\theta}{2}) \frac{\Delta B_{geo}}{2} \quad (2)$$

$$\Delta q_{hkl} = ((\Delta q_{hkl})^2 - (\Delta q_{res})^2)^{1/2} \quad (3)$$

Here, ΔB_{geo} is the geometric broadening, 2θ is the Bragg angle, w is the beam footprint in GIWAXS measurement, L is the sample-to-detector distance and λ is the X-ray wavelength.

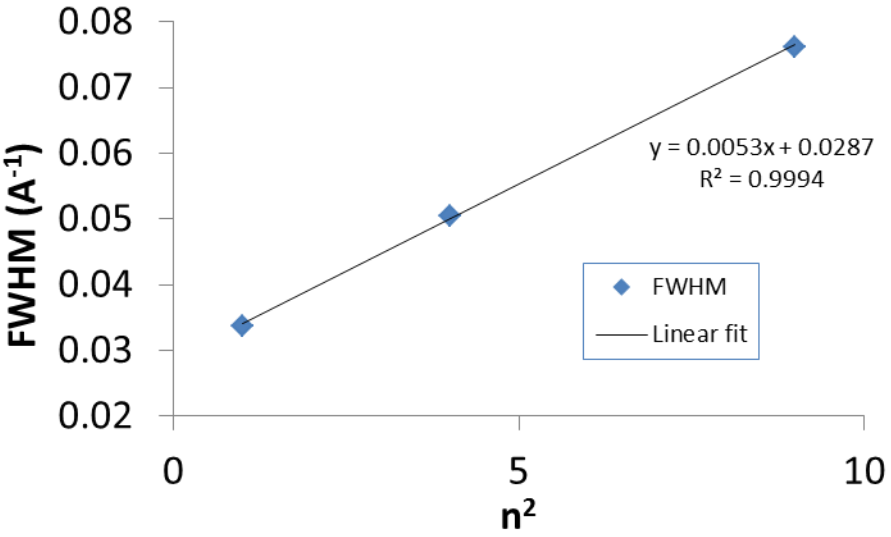

Figure S2: An example of Williamson-Hall analysis

After correcting the FWHM of each (*h*00) peaks, we perform a simple linear fit of FWHM as a function of h^2, an example of which is shown in Figure S2 above. We extract the disorder parameter from the slope *a* of the fit and extract the crystallite size L_c from the intercept *b* according to:

$$L_C = 0.886 \frac{2\pi}{b} \quad (4)$$

3) Spano and Gierschner analysis

The aggregate length (or conjugation length) was calculated using a combination of theoretical works by Spano and Gierschner et al. First, the absorption spectra were fit using the following Spano equation in order to extract the exciton bandwidth *W*. Here, *A* is the absorption of the aggregates as a function of photon energy, *E*; *S* is the Huang-Rhys factor, representing the overlap between vibrational states and assumed to be 1; *m* corresponds to different energy levels and E_p = 0.179 eV is the energy of C=C symmetric stretch mode.[3] [3,4]

$$A_{aggregate} \propto \sum_{m=0} \left(\frac{S^m}{m!}\right) \times \left(1 - \frac{We^{-S}}{2E_p} \sum_{n \neq m} \frac{S^n}{n!(n-m)}\right)^2 \times e^{\frac{(E - E_0 - mE_p - \frac{1}{2}WS^m e^{-S})^2}{2\sigma^2}} \quad (5)$$

The conjugation length was then derived by theoretical work of Gierschner et al who calculated the exciton coupling as a function of repeating unit.[5] Since Gierschner et al. calculated the coupling in polythiophene without any side chain, we corrected by a factor of 0.8 in order to account for the side-chain effect in P3HT, as pointed out by Scharsich et al.[6] Figure S3 shows the polynomial model used to extrapolate repeating units and conjugation length corresponding to each value of *W*.

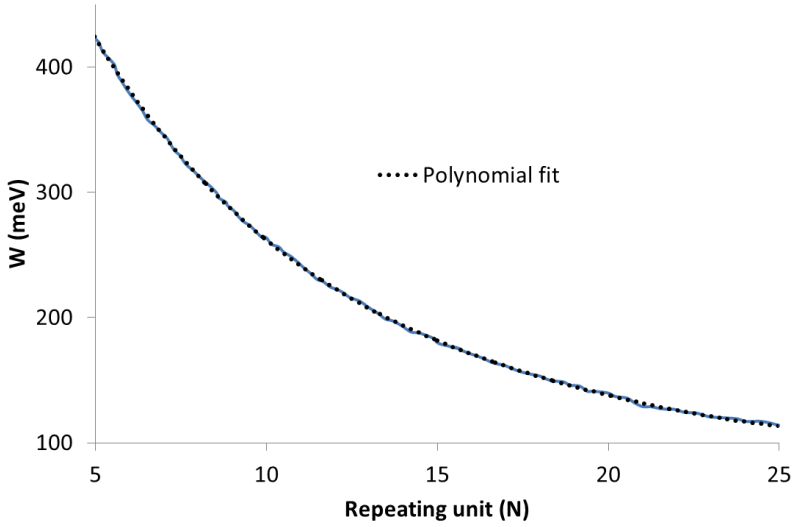

Figure S3: The exciton bandwidth *W* as a function of the number of thiophene across the polymer backbone.

4) Effect of benzyl alcohol (BnOH) on the absorption spectra

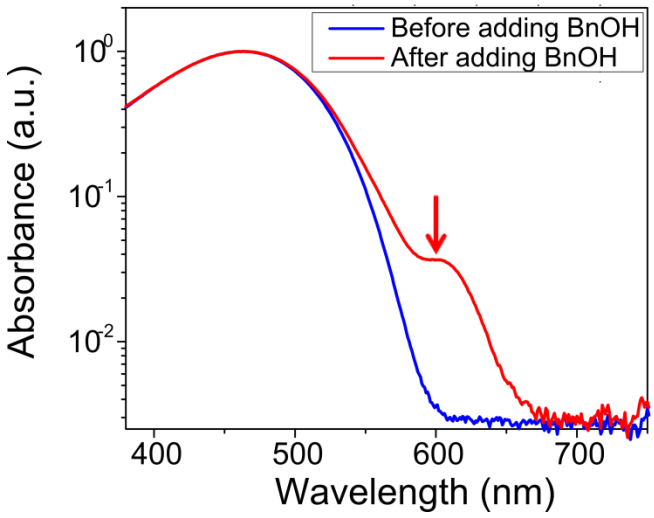

Figure S4: UV-vis absorption spectra of dilute P3HT solutions before and after addition of 33 vol % of BnOH.

BnOH can also promote chain aggregations in P3HT solution due to the poor solubility of P3HT in it. This is evidenced by the UV-vis absorption spectra measurement of dilute P3HT solution before and after adding BnOH, as plotted in Figure S4. The appearance of the aggregate shoulder at ca. 610 nm upon adding 33 vol % BnOH (the same ratio we use to make emulsion) as indicated by the arrow in Figure S2 indicates the formation of π-stack aggregates within the solution.

5) Effect of regioregularity and PDI of P3HT on absorption spectra

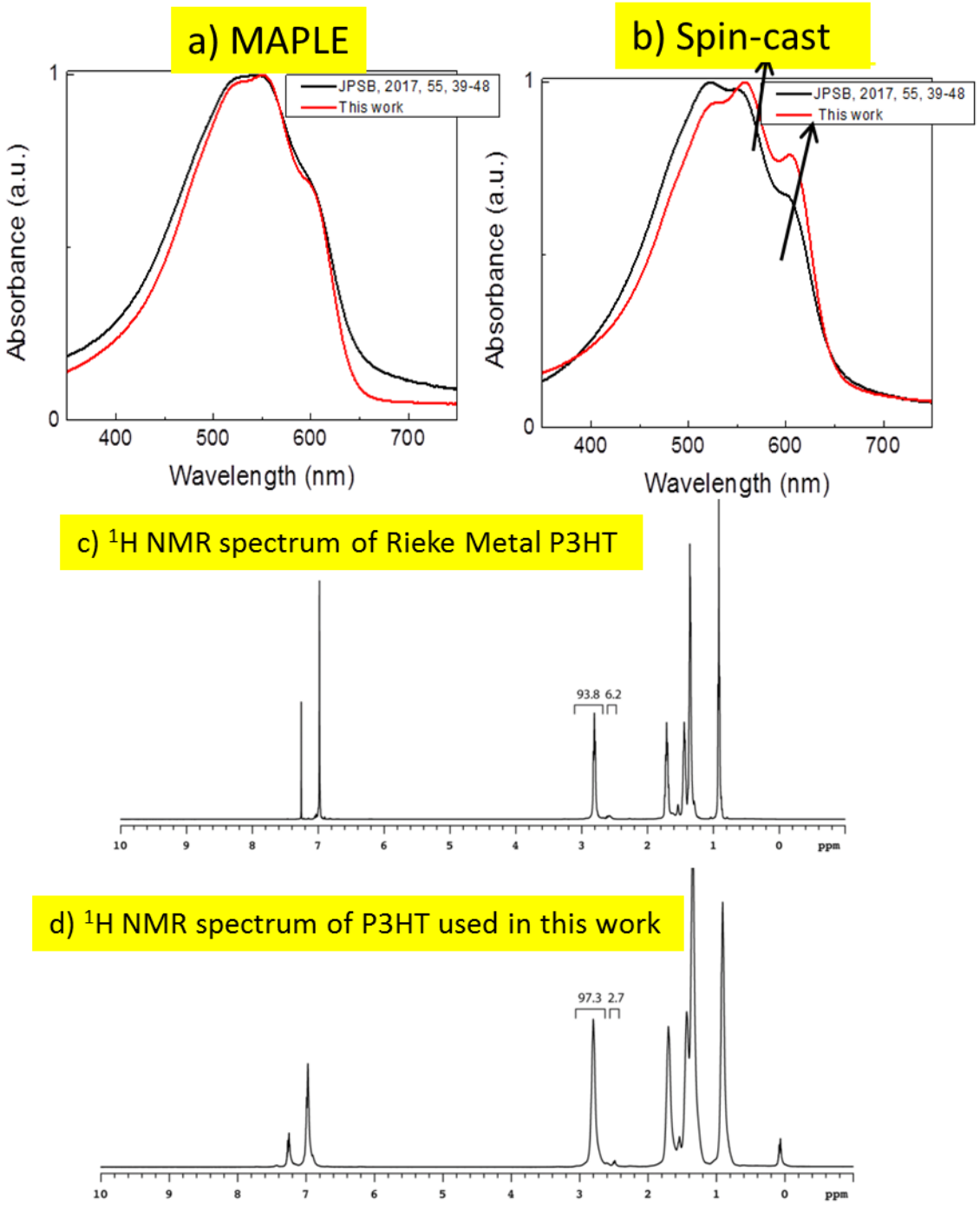

Figure S5: UV-vis absorption spectra of (a) MAPLE and (b) spin-cast films for two different P3HT batches: One used in our previous work JPSB, 2017, 55, 39-48 and one used in our current

work. The ^{1}H NMR spectra of the (c) commercial Rieke Metal P3HT and (d) P3HT batch used in this work.

It is important to note that in this work, we do not see the same conjugation length for MAPLE and spin-cast samples at high MW as observed in our previous publication.[7,8] It could be that the P3HT batch we used in this work has higher quality than the commercial one we used in previous publications. While the MW of the two batches are almost the same (ca. 20 kDa), the regioregularity and $Đ$ of the batch used here are 97% and 1.4, whereas those of Riekei Metal used in previous works were 94% and 2.7. (See the ^{1}H NMR spectra in Figure S5). It can be seen from the absorption spectra that spin-cast film from this work shows stronger aggregate shoulders in absorption spectra. MAPLE films on the other hand show negligible changes of absorption spectra between the two batches. This observation suggests that MAPLE structure is rather insensitive to $Đ$ or regioregularity.

6) TFT transfer characteristics

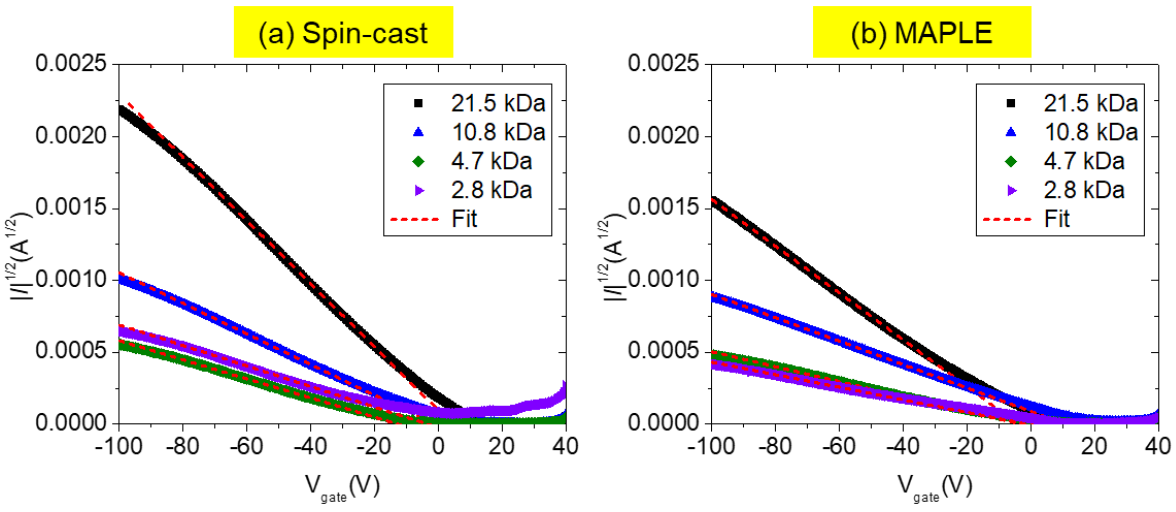

Figure S6: Transfer characteristics curve of (a) spin-cast and (b) MAPLE-deposited samples at different MWs. The dashed red lines represent the linear fit to the transfer curves from which the hole mobilities were extracted.

7) References

(1) Smilgies, D. M. *J. Appl. Crystallogr.* **2009**, *42* (6), 1030–1034.

(2) Dong, B. X.; Strzalka, J.; Jiang, Z.; Li, H.; Stein, G. E.; Green, P. F. *ACS Appl. Mater. Interfaces* **2017**, *9*, 44799–44810.

(3) Spano, F. C. *J. Chem. Phys.* **2005**, *122* (23), 234701.

(4) Spano, F. C.; Silva, C. *Annu. Rev. Phys. Chem.* **2014**, *65*, 477–500.

(5) Gierschner, J.; Huang, Y.-S.; Van Averbeke, B.; Cornil, J.; Friend, R. H.; Beljonne, D. *J. Chem. Phys.* **2009**, *130* (4), 44105.

(6) Scharsich, C.; Lohwasser, R. H.; Sommer, M.; Asawapirom, U.; Scherf, U.; Thelakkat, M.; Neher, D.; Köhler, A. *J. Polym. Sci. Part B Polym. Phys.* **2012**, *50* (6), 442–453.

(7) Dong, B. X.; Li, A.; Strzalka, J.; Stein, G. E.; Green, P. F. *J. Polym. Sci. Part B Polym. Phys.* **2017**, *55* (1), 39–48.

(8) Li, A.; Dong, B. X.; Green, P. *MRS Commun.* **2015**, *5* (4), 593–598.